The equivalent of a thallium binding residue from an archeal homolog controls cation interactions in brain glutamate transporters

Shlomit Teichman[1], Shaogang Qu[1], and Baruch I. Kanner[2]

Department of Biochemistry, Hebrew University Hadassah Medical School, P.O. Box 12272, Jerusalem 91120, Israel

Edited by H. Ronald Kaback, University of California, Los Angeles, CA, and approved July 10, 2009 (received for review April 27, 2009)

Glutamate transporters maintain low synaptic concentrations of neurotransmitter by coupling uptake to flux of other ions. Their transport cycle consists of two separate translocation steps, namely cotransport of glutamic acid with three Na^+ followed by countertransport of K^+. Two Tl^+ binding sites, presumed to serve as sodium sites, were observed in the crystal structure of a related archeal homolog and the side chain of a conserved aspartate residue contributed to one of these sites. We have mutated the corresponding residue of the eukaryotic glutamate transporters GLT-1 and EAAC1 to asparagine, serine, and cysteine. Remarkably, these mutants exhibited significant sodium-dependent radioactive acidic amino acid uptake when expressed in HeLa cells. Reconstitution experiments revealed that net uptake by the mutants in K^+-loaded liposomes was impaired. However, with Na^+ and unlabeled L-aspartate inside the liposomes, exchange levels were around 50–90% of those by wild-type. In further contrast to wild-type, where either substrate or K^+ stimulated the anion conductance by the transporter, substrate but not K^+ modulated the anion conductance of the mutants expressed in oocytes. Both with wild-type EAAC1 and EAAC1-D455N, not only sodium but also lithium could support radioactive acidic amino acid uptake. In contrast, with D455S and D455C, radioactive uptake was only observed in the presence of sodium. Thus the conserved aspartate is required for transporter-cation interactions in each of the two separate translocation steps and likely participates in an overlapping sodium and potassium binding site.

cation binding site | obligate exchange mutant | sodium selectivity

Glutamate transporters are key elements in the termination of the synaptic actions of the neurotransmitter and keep its synaptic concentrations below neurotoxic levels. Glutamate transport is an electrogenic process (1, 2) consisting of two sequential translocation steps: (*i*) Cotransport of the neurotransmitter with three sodium ions and a proton (3, 4) and (*ii*) the countertransport of one potassium ion (5–7). The mechanism involving two half-cycles (Fig. 1*A*) is supported by the fact that mutants impaired in the interaction with potassium are "locked" in an obligatory exchange mode (7, 8). Glutamate transporters mediate two distinct types of substrate-induced steady-state current: An inward-rectifying or "coupled" current, reflecting electrogenic sodium-coupled glutamate translocation, and an "uncoupled" sodium-dependent current, which is carried by chloride ions and further activated by substrates of the transporter (9–11). Nontransportable substrate analogs, expected to "lock" the transporter in an outward-facing conformation (stippled part of Fig. 1*A*), are not only competitive inhibitors of the two types of substrate-induced current, but also inhibit the basal sodium-dependent anion conductance (12, 13).

Recently a high-resolution crystal structure of a glutamate transporter homolog, Glt_{Ph}, from the archeon *Pyrococcus horikoshii* was published (14). It forms a trimer with a permeation pathway through each of the monomers, indicating that the monomer is the functional unit. This is also the case for the eukaryotic glutamate transporters (15–18). The membrane topology of the monomer (14) is quite unusual, but is in excellent agreement with the topology inferred from biochemical studies (19–21). The monomer contains eight transmembrane domains (TM) and two oppositely oriented reentrant loops, one between domains 6 and 7 (HP1) and the other between domains 7 and 8 (HP2). TMs 1–6 form the outer shell of the transporter monomer, whereas TMs 7 and 8 and the two reentrant loops participate in the formation of the binding pocket of Glt_{Ph} (14, 22). Importantly, many of the amino acid residues of the transporter, inferred to be important in the interaction with sodium (23, 24), potassium (7, 8), and glutamate (25, 26) are facing toward the binding pocket.

Because of the limited resolution of the Glt_{Ph} structure, Tl^+ ions, which exhibit a robust anomalous scattering signal, have

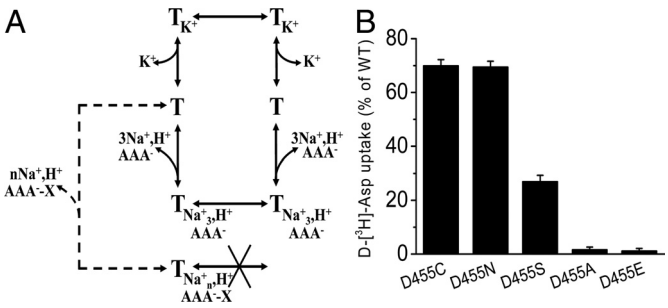

Fig. 1. Transport cycle and transport activity of D455 mutants. (*A*) Transport cycle of GLT-1 and other eukaryotic glutamate transporters (full lines). After binding of sodium, acidic amino acid (AAA^-), and a proton from the extracellular medium (left), the outward-facing substrate-loaded translocation complex is formed. After the closing of the external gate and the opening of the internal one, the substrate and cotransported ions dissociate into the cytoplasm (right). Subsequently, intracellular potassium enters the binding pocket. After the internal gate closes, the external gate opens and potassium is released into the extracellular medium, completing net influx. Net efflux, observed at elevated extracellular potassium concentrations, proceeds via reversal of the above steps. Exchange involves reversible translocation via the glutamate half-cycle and does not require potassium. When a bulky nontransportable analog (AAA^--X) binds from the extracellular medium together with sodium [the stoichiometry (*n*) is unknown], the transporter remains locked in the outward-facing conformation (dashed line) because translocation cannot proceed. (*B*) The Cys-less GLT-1 and the indicated mutants in the Cys-less GLT-1 background were expressed in HeLa cells, and transport was measured as described in the *Materials and Methods*. The data are given as percent of activity of Cys-less GLT-1.

Author contributions: B.I.K. designed research; S.T. and S.Q. performed research; S.T., S.Q., and B.I.K. analyzed data; and S.T., S.Q., and B.I.K. wrote the paper.

The authors declare no conflict of interest.

This article is a PNAS Direct Submission.

[1]S.T. and S.Q. contributed equally to this manuscript.

[2]To whom correspondence should be addressed. E-mail: kannerb@cc.huji.ac.il.

This article contains supporting information online at www.pnas.org/cgi/content/full/0904625106/DCSupplemental.

been used in an attempt to visualize the sodium sites (22). One of the bound Tl^+ sites was found to be buried just under HP2 and seemed to have only four coordinating main chain carbonyl oxygens from TM7 and HP2. The other Tl^+ site was buried deeply within the protein, coordinated by three main chain carbonyl oxygens from TM7 and TM8 as well as the two carboxyl oxygens of a conserved TM8 aspartate residue (Asp-405) and possibly a hydroxyl oxygen of a HP1 serine residue (22) (see Fig. S1 for the proximity of Asp-405 to the substrate and the thallium ions bound to the transporter). Nevertheless, there is uncertainty on assumption that Tl^+ faithfully reports on Na^+ because in contrast to Na^+, Tl^+ could not support transport (22). During the functional analysis of TM8 mutants of the glial glutamate transporter GLT-1 (27) and of the neuronal glutamate transporter EAAC1 (28), also known as EAAT2 and EAAT3, respectively (29), we found to our surprise that mutants of the corresponding aspartate residues (Asp-485 and Asp-455, respectively) retained the ability to mediate sodium dependent uptake of radioactive acidic amino acids. Here we present evidence that this aspartate residue is required for transporter-cation interactions in each of its two separate translocation steps. From now on this residue is referred to as Asp-455, regardless if the background is GLT-1 or EAAC1.

Results

Transport of D-[^{3}H]-Aspartate by Asp-455 Mutants. Upon expression in HeLa cells, several Asp-455 mutants in the background of the Cysteine-less GLT-1 (C-less GLT-1) (19) exhibited significant levels of D-[^{3}H]-Aspartate transport. This was especially true for the D455N and D455C mutants, whereas lower yet significant transport was observed with D455S (Fig. 1*B*). On the other hand, very little D-[^{3}H]-Aspartate transport was seen with the mutants D455E and D455A mutants (Fig. 1*B*). In contrast to D455E, the lack of transport by D455A was not due to reduced transporter levels at the plasma membrane, as determined by suface-biotinylation (Fig. S2). In the case of the D455C mutant, but not of the C-less GLT-1, the radioactive uptake was inhibited by 45.5 ± 5.4% by 0.25 mM the permeant sulfhydryl reagent N-ethylmaleimide (NEM) (Fig. S3), but no inhibition was observed with the impermeant reagent [2-(trimethylammonium) ethyl]methanethiosulfonate (MTSET) (data not shown). The inhibition by NEM was not modulated by substrate or nontransportable substrate analogs (Fig. S3), expected to increase the proportion of inward- or outward-facing transporters, respectively. When the corresponding mutants of the glutamate transporter EAAC1 were examined, significant D-[^{3}H]-Aspartate transport was observed with the D455N, D455C, and D455S mutants, and the same was true for transport of L-[^{3}H]-Aspartate and L-[^{3}H]-Glutamate for these mutants in either EAAC-1 or GLT-1 background (Fig. S4). On the other hand, no measurable radioactive uptake of D- and L-aspartate and of L-glutamate was detected with the D455E and D455A mutants (Fig. S4).

Because HeLa cells, like many other cell types, have high endogenous levels of glutamate and aspartate, radioactive uptake of acidic amino acids does not necessarily reflect net flux, but can also be due to exchange of the labeled extracellular substrate and its unlabeled intracellular counterpart, via the lower half-cycle depicted in Fig. 1*A*. To distinguish between these two possibilities, the mutant transporters expressed in HeLa cells were solubilized and reconstituted into liposomes. Upon detergent removal in the presence of potassium phosphate, the internal medium of the liposomes contains potassium, but not the acidic amino acids endogeneous to the HeLa cells (7). Under these conditions, the radioactive D-[^{3}H]-Aspartate uptake by the liposomes inlaid with C-less GLT-1, represents net flux, involving the sodium-coupled substrate translocation step followed by the potassium-dependent reorientation step (lower and upper half-cycles depicted in Fig. 1*A*). Net D-[^{3}H]-Aspartate flux by the D455N, D455C, and D455S mutants ranged between 1–3% of that of C-less GLT-1, and similar observations were made on the corresponding mutants of the glutamate transporter EAAC1 (Fig. 2, gray bars). On the other hand, when the liposomes contained internal sodium phosphate and 10 mM L-aspartate (exchange conditions), the levels of exchange were around 50–90% of that of wild-type (WT), regardless if GLT-1 or EAAC1 was monitored (Fig. 2, black bars). Similar results were obtained with L-[^{3}H]-glutamate (Fig. S5). Even after reconstitution, no activity of D455E was observed (Fig. 2), indicating that the lack of activity of this mutant in intact cells (Fig. 1*B*) is not solely due to a targeting defect.

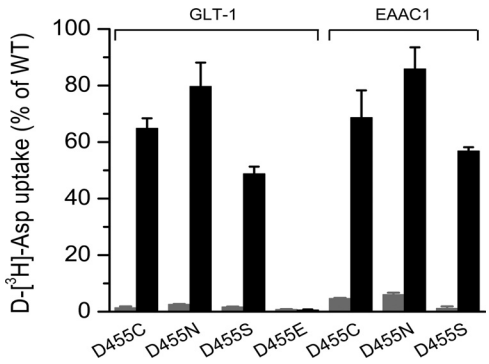

Fig. 2. Uptake of D-[^{3}H]-aspartate in proteoliposomes. Proteoliposomes were prepared from HeLa cells expressing the indicated mutants in Cys-less GLT-1 or EAAC1, respectively, as described in the *Materials and Methods* using 10 μL proteoliposomes, which were diluted into 360 μL 0.15 M NaCl supplemented with 1 μCi of D-[^{3}H]-aspartate and 2.5 μM valinomycin for each triplicate time point (10 min). The data are given as percent of activity of the corresponding WT. The ''in''-medium contained either 0.12 M KPi, pH 7.4 (net flux, gray bars), or 0.12 M NaPi, pH 7.4, plus 10 mM L-aspartate (exchange, black bars).

Currents by Asp-455 Mutants. Previously characterized mutants, which are "locked" in the exchange mode, do not exhibit the "coupled" current, but nevertheless retain the substrate-induced anion conductance (7, 8, 30). Because EAAC1 expresses in *Xenopus laevis* oocytes much better than GLT-1, the electrophysiological experiments were conducted with the mutants in the EAAC1 background. In EAAC1-WT, replacing 10% of the external NaCl by NaSCN almost fully abolished the inward-rectification of the currents induced by L-aspartate (Fig. 3*A*). This is due to the fact that the permeability of SCN^- through the transporter-mediated anion conductance is around 70-fold of the permeability of Cl^- (31) and as a result, outward currents, reflecting the entry of the permeant anion at positive potentials, become visible in the presence of SCN^- (Fig. 3*A*). Such currents were not induced by GABA, which is not a substrate of the transporter. The nontransportable substrate analog (blocker) D,L-threo-β-benzoylaspartate (TBOA) blocked the currents (the subtraction of currents in the absence of blocker from those in its presence yields currents in the opposite direction), particularly at positive potentials (Fig. 3*A*).

The anion currents by D455C and D455S were suppressed rather than stimulated by L-aspartate (Figs. 3 *B* and *C* and Fig. S6). In the absence of SCN^-, the L-aspartate-induced currents were very small but had the same voltage dependence as in its presence (Fig. 3 *B* and *C*), rather than the inwardly rectifying "coupled" current observed with WT (Fig. 3*A*). A similar suppression of the currents was also observed with L-glutamate and D-aspartate, and the apparent affinity for the three acidic amino acids was higher than or similar to that in EAAC1-WT (30) (Table S1). In the D455N mutant, L-aspartate stimulated

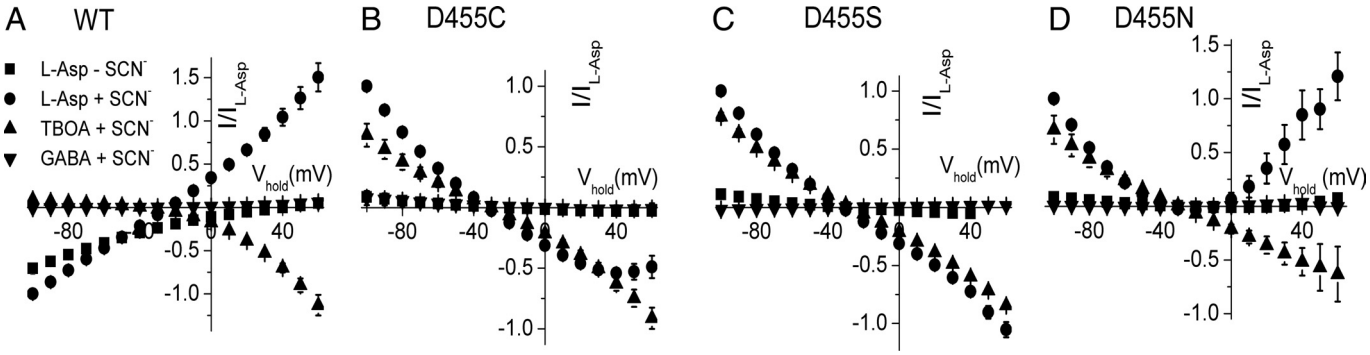

Fig. 3. Currents in oocytes expressing WT and D455 mutants. Difference records obtained by subtraction of currents by oocytes expressing EAAC1-WT (*A*) or the indicated mutants (*B–D*) in the indicated perfusion medium from those in the same medium but in the presence of of either 2 mM L-Aspartate (filled squares, filled circles), 10 μM D,L- TBOA (filled triangles), or 2 mM GABA (inverted filled triangles). The perfusion medium was either ND96 (-SCN^-, filled squares) or ND96, where 9.6 mM NaCl was replaced by an equimolar concentration of NaSCN (+SCN^-,filled circles,filled triangles,inverted filled triangles). Pulses were 250 ms in duration in 10-mV increments to potentials between −100 mV to +60 mV from a holding potential of −25 mV. Data were normalized to the L-aspartate-elicited current, in the NaSCN-containing medium at −100 mV, and plotted against the holding potential. Values are mean ± SE of three to nine repeats. Absolute values for L-aspartate-induced currents at −100 mV in NaSCN 9.6 ranged from 112 to 1299 nA in WT, from 262 to 569 nA in D455C, from 257 to 1187 nA in D455S, and from 559 to 1604 nA in D455N.

the anion conductance at positive potentials, but inhibited at negative potentials (Fig. 3*D*). Also with this mutant, the currents in the absence of SCN^- were much reduced, but again their voltage-dependence was unchanged (Fig. 3*D*). Despite the complex effect of L-aspartate on the currents by D455N, the blocker TBOA suppressed the anion conductance both at positive and negative potentials (Fig. 3*D*), similar to its effect on the other mutants (Fig. 3*B* and *C*) and EAAC1-WT (Fig. 3*A*). The apparent affinity for sodium of the three mutants, using the currents modulated by 2 mM L-aspartate as an assay, was similar to that of EAAC-1-WT (24) (Table S1).

Besides the biochemical approach used to probe the interaction of the Asp-455 mutants with potassium (Fig. 2), we have also examined this interaction using electrophysiological measurements. In oocytes expressing glutamate transporters, elevation of external potassium induces reverse transport of endogeneous acidic amino acids (Fig. 1*A*), and this results in the activation of the transporter-mediated anion conductance (7). This was observed with EAAC1-WT (Fig. 4*A*), but not with the D455C, D455S, and D455N mutants (Figs. 4 *B–D*).

Sodium-Selectivity of Radioactive Uptake. Our observations thus far can be explained by the idea that Asp-455 is important for the interaction of the transporter with potassium, so that mutants at this position only can execute the sodium-coupled glutamate translocation step (lower half cycle of Fig. 1*A*). To explore the question if the sodium interaction of the mutants is altered as well, we examined the cation selectivity of the substrate translocation step. Two of the three sodium ions required for substrate translocation by GLT-1 apparently can be replaced by lithium (32). On the other hand, in EAAC1, lithium can support substrate transport in the complete absence of sodium, suggesting that in EAAC1, all three sodium ions can be replaced by lithium (24). This difference between the two isotransporters appears to be due to a difference of a single amino acid residue located at the tip of reentrant loop HP2 (23, 24). Therefore we examined the ability of lithium to support substrate transport in the mutants in the background of EAAC1. The initial rate of L-[^{3}H]-aspartate transport by EAAC1-WT in the presence of lithium was 21.7% ± 0.6% of that in the presence of sodium (Fig. 5). This ratio was even higher with D455N, but in the two other mutants, the ability of lithium to replace sodium was markedly impaired (Fig. 5). In EAAC1-WT, lithium was less effective in replacing sodium when transport of L-[^{3}H]-glutamate or of D-[^{3}H]-aspartate was measured (Fig. 5). Nevertheless, the behavior of the mutants was similar to that observed with L-[^{3}H]-aspartate transport; lithium was at least as effective with D455N as with WT, but much less effective with D455C and D455S (Fig. 5). This behavior by the mutants was similar when the apparent affinity for sodium was measured using D-[^{3}H]-aspartate transport as an assay. In the case of D455N, the apparent affinity for sodium was higher than that of EAAC1-WT, whereas with

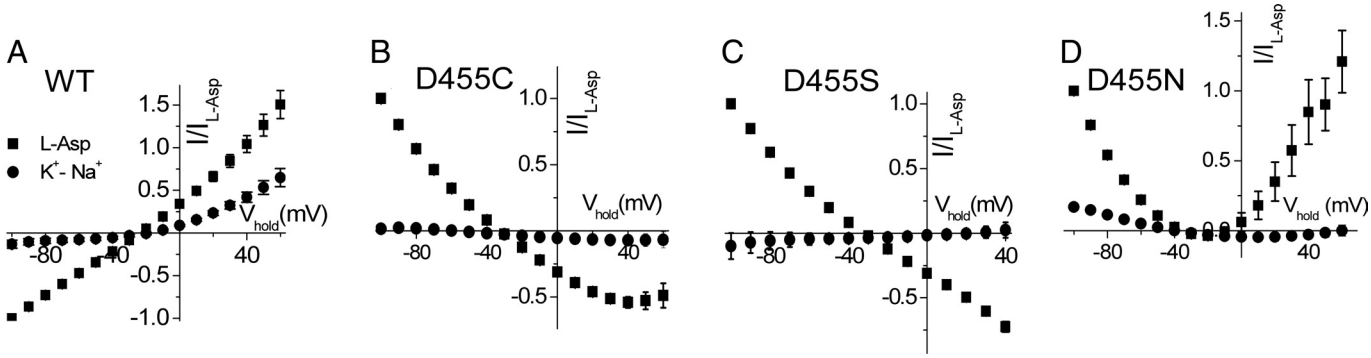

Fig. 4. Effect of extracellular potassium on the currents by WT and Asp-455 mutants. Difference records obtained by subtraction of currents in the NaSCN containing medium (as in Fig. 3) from those in the same medium containing 2 mM L-aspartate (filled squares) or from those in KSCN [the same solution, but KSCN (9.6 mM) replaced NaSCN, filled circles] using the same oocytes as in Fig. 3.

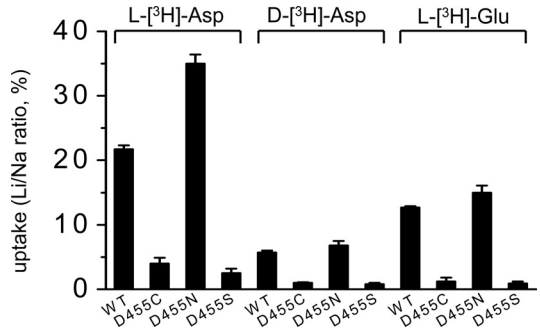

Fig. 5. Cation selectivity of uptake by Asp-455 mutants in intact HeLa cells. EAAC1-WT and the Asp-455 mutants were expressed in HeLa cells, and transport of L- and D-[^{3}H]-aspartate and L-[^{3}H]-glutamate was measured in lithium- and sodium-containing transport solutions. The data are given the ratio of transport in the presence of lithium to that in the presence of sodium (%).

D455C and especially with D455S, it was lower (Fig. S7). The cooperativity with regard to sodium was not changed much in the mutants; the Hill coefficients for EAAC1-WT, D455N, D455C, and D455S were 1.63 ± 0.13, 1.34 ± 0.10, 1.42 ± 0.08, and 1.60 ± 0.13, respectively. Even though the glutamate and alanine substitution mutants were devoid of transport in the presence of sodium, we also measured it in the presence of lithium. However transport of L-[^{3}H]-aspartate by D455E and D455A could also not be observed under these conditions (data not shown).

Discussion

Mutations of Asp-455 of GLT-1 and EAAC1 lead to a defective interaction with potassium (Figs. 2 and 4), yet sodium-coupled substrate translocation remains relatively intact (Figs. 1*B* and 2). Because of these observations, we were initially somewhat skeptical on the postulated role of this residue in sodium binding (22), at least in the eukaryotic glutamate transporters. However, the ability of lithium to replace sodium in radioactive transport by the EAAC1 mutants D455S and D455C was impaired (Fig. 5), as if the mutation has destroyed the ability of lithium to replace sodium at one of the three sites, without impairing the binding of sodium itself. A similar phenomenon has been previously observed at other EAAC1 positions, which presumably affect the cation selectivity at different sodium sites (24). An alternative explanation could have been that the mutations have resulted in a decrease of the sodium:substrate stoichiometry, rendering the site influenced by Asp-455 unnecessary for transport. Because the mutants are locked in an exchange mode, we cannot experimentally test this alternative. This is because one or more sodium ions can bind before substrate on the extracellular side (33, 34), and all three sodium ions unbind after the substrate on the intracellular side (35). Therefore many labeled substrate molecules can be exchanged for intracellular unlabeled substrate molecules without any accompanying sodium translocation. Nevertheless, such a change in stoichiometry is highly unlikely, because in such a scenario, transport still would be expected to be possible in the sole presence of lithium. Thus our results with the Asp-455 mutants are compatible with the prediction that this residue participates in the coordination of one of the cotransported sodium ions (Na 1), based on the GltPh structure (22) and on molecular simulations based on this structure (36).

Lithium can still support transport in the D455N mutant (Fig. 5), but potassium interaction is disrupted in this mutant (Figs. 2 and 4*D*). Thus the role of the conserved aspartate residue in the interaction with potassium is more stringent than that with sodium. It is noteworthy that when the corresponding aspartate of GltPh was mutated to asparagine, the thallium interaction at site 1 was lost (22), and our observations are in line with a very recent publication indicating that Tl^+ is more efficient in mimicking K^+ than Na^+ when interacting with the mammalian protein (37). Moreover, our results are also in harmony with the conclusion that the D454N mutant in rat EAAC1, which is equivalent to D455N studied here, can still interact with sodium and substrate (38, 39). The fact that Asp-455 is required for transporter cation interactions in each of its two separate translocation steps, suggests that this residue may participate in an overlapping sodium and potassium binding site. This suggestion is based on the assumption that the structure of the active center of Glt_{Ph} is very similar to that of GLT-1 and EAAC1. While all of the available evidence supports this assumption (14, 22, 25, 26, 40), final proof for a direct interaction of Asp-455 with sodium and potassium will have to await high-resolution crystal structures of the mammalian glutamate transporters. Thus at the present time, indirect effects of the mutations of Asp-455 at remote cation binding sites cannot be totally excluded. Overlapping cation sites also have been implicated in the sodium-potassium pump (41–43), which interestingly also operates with two sequential half-cycles for sodium and potassium pumping, respectively. Two other sites in the eukaryotic glutamate transporters have been suggested to be closely linked to interaction with both sodium and potassium (7, 8, 30, 44). The transport cycle requires the cotransport with three sodium ions and countertransport of only one potassium ion. One of the possible scenarios is that the potassium ion hops through the transporter at or near each of the three binding sites for sodium. On the other hand, it should be noted that one of the other residues implicated in potassium interaction, was later proposed to interact with the cotransported proton and not necessarily with potassium (45), so it is also possible that there just is a single potassium binding site.

Transport by mutant D455C, in the background of the Cys-less GLT-1, was inhibited by the membrane permeant sulfhydryl reagent NEM (Fig. S3), which reacts with the thiolate anion and therefore the reactivity of D455C reflects accessibility from the aqueous medium. However, this inhibition was not modulated by conditions favoring the extracellular- or intracellular-facing conformations of the transporter (Fig. S3), consistent with the idea that the engineered cysteine is located on the translocation pathway and thus can be reached via an aqueous pathway from the extracellular as well as from the intracellular side of the membrane in different conformations of the transporter.

Assuming that Asp-455 indeed directly ligands sodium and potassium during sodium-coupled substrate translocation and reorientation of the substrate-free transporter, respectively, its precise role in the geometry of these sites yet remains to be clarified. Because glutamate has a longer side-chain than aspartate, the fact that the D455E mutant has an intrinsic defect in activity indicates that the positioning of the side-chain oxygens is crucial. Whereas both asparagine and serine have oxygen containing side-chains, cysteine, being only very slightly polar, is a borderline ligand for cations. However, the substrate carboxylate is also nearby, so it is possible that the sodium should still have enough electrostatic stabilization that a mutation to cysteine would not be enough to prevent binding. In fact, when the conserved aspartate residue is mutated, this carboxylate of the substrate may actually become closer to the putative bound sodium, because of the elimination of a negative charge at the binding pocket. It has been suggested that the cotransported solutes can interact functionally in the binding pocket of the glutamate transporters (46), and also in the present study, we show that the ability of lithium to replace sodium depends on the nature of the acidic amino acid substrate (Fig. 5). An attractive explanation is suggested by the very recent finding of a third potential sodium site by valence mapping of the predicted cation binding sites in the Glt_{Ph} structure (47); namely the β-carboxyl of the bound aspartate, and even more so the γ-carboxyl group of glutamate would be very close to this sodium.

Our electrophysiological data on the Asp-455 mutants also indicate that the interaction of substrate with the binding pocket is altered. Substrates increase the anion conductance in EAAC1-WT, but suppressed it in the D455C and D455S mutants (Fig. 3). In the case of D455N, stimulation and inhibition were observed at positive and negative potentials, respectively (Fig. 3), indicating that multiple substrate-bound conformations can gate the anion conductance in this mutant. The blocker TBOA suppressed the anion conductance in EAAC1-WT and all of the mutants (Fig. 3). Since substrate can still be translocated in the Asp-455 mutants, it is obvious that inhibition of the anion conductance is not necessarily an indication of the blocked state. It will be exciting to address the mechanistic aspects of these issues in the future, but this can be addressed only after the molecular details of the anion conduction pathway through the transporter become available.

Materials and Methods

Generation and Subcloning of Mutants. The C-terminal histidine-tagged versions of Cys-less rat GLT-1 (19) and rabbit EAAC1 (28, 48) in the vector pBluescript SK$^-$ (Stratagene) were used as a parent for site-directed mutagenesis (49, 50). This was followed by subcloning of the mutations into the starting parent Cys-less GLT-1 construct or into the his-tagged EAAC1, residing in the oocyte expression vector pOG$_1$ (48), respectively, using unique restriction enzymes. The subcloned DNA fragments were sequenced between these unique restriction sites.

Cell Growth and Expression. HeLa cells were cultured (51), infected with the recombinant vaccinia/T7 virus vTF$_{7-3}$ (52), and transfected with the plasmid DNA harboring the WT or mutant constructs or with the plasmid vectors alone (51). Transport of D-[^{3}H]-aspartate or other radiolabeled substrates was done as described (49). Usually D-[^{3}H]-aspartate in transport assays, because of the low background values obtained in HeLa cells, transfected with the vector alone. Briefly, HeLa cells were plated on 24-well plates and washed with transport medium containing 150 mM NaCl/5 mM KPi, pH 7.4. Each well was then incubated with 200 μL transport medium supplemented with 0.4 μCi of the tritium-labeled substrates and incubated for 3 or 10 min, followed by washing, solubilization of the cells with SDS, and scintillation counting. Where necessary, the NaCl was replaced by LiCl or choline chloride, both during washing and transport. Surface biotinylation (53) in HeLa cells, as well as solubilization of transporters expressed in HeLa cells, their reconstitution, and analysis by transport (7, 27), were done as described. Exchange data are presented as net exchange after subtracting the values obtained on proteoliposomes not containing 10 mM L-aspartate, but only 0.12 M sodium phosphate, pH 7.4. Protein was determined by Lowry's method (54).

Expression in Oocytes and Electrophysiology. cRNA was transcribed using mMESSAGE-mMACHINE (Ambion), injected into *Xenopus laevis* oocytes, and maintained as described (24). Oocytes were placed in the recording chamber, penetrated with two agarose-cushioned micropipets (1%/2M KCl, resistance varied between 0.5 and 3 mΩ), voltage-clamped using GeneClamp 500 (Axon Instruments), and digitized using Digidata 1322 (both controlled by the pClamp9.0 suite; Axon Instruments). Voltage jumping was performed using a conventional two-electrode voltage clamp as described previously (48). The standard buffer, termed ND96, was composed of 96 mM NaCl, 2 mM KCl, 1.8 mM $CaCl_2$, 1 mM $MgCl_2$, 5 mM Na-HEPES, pH 7.5. The composition of other perfusion solutions is indacted in the figure legends. Offset voltages in chloride substitution experiments were avoided by use of an agarose bridge (1%/2M KCl) that connected the recording chamber to the Ag/AgCl ground electrode.

Data Analysis. All current-voltage relations (Figs. 3 and 4) represent steady-state substrate-elicited net currents [($I_{buffer+substrate}$) $-$ (I_{buffer})] and were analyzed by Clampfit version 8.2 or 9.0 (Axon instruments). Because of the variability in expression level within and between different oocyte batches, the data have been normalized as indicated in the figure legends. Kinetic parameters were determined by nonlinear fitting to the generalized Hill equation using the build-in functions of Origin 6.1 (Microcal). For determination of apparent affinity for substrate, I_{max} and $K_{0.5}$ were allowed to vary, and the value of n_H was fixed at 1, whereas this parameter was allowed to vary for the calculation of the apparent affinity for sodium.

ACKNOWLEDGMENTS. We thank Lucy Forrest for helpful discussions. This work was supported by the National Institute of Neurological Disorders and Stroke (NINDS), National Institutes of Health Grant NS16708 and by U.S.-Israel Binational Science Foundation Grant 2007051.

1. Kanner BI, Sharon I (1978) Active transport of L-glutamate by membrane vesicles isolated from rat brain. *Biochemistry* 17:3949–3953.
2. Brew H, Attwell D (1987) Electrogenic glutamate uptake is a major current carrier in the membrane of axolotl retinal glial cells. *Nature* 327:707–709.
3. Zerangue N, Kavanaugh MP (1996) Flux coupling in a neuronal glutamate transporter. *Nature* 383:634–637.
4. Levy LM, Warr O, Attwell D (1998) Stoichiometry of the glial glutamate transporter GLT-1 expressed inducibly in a Chinese hamster ovary cell line selected for low endogenous Na+-dependent glutamate uptake. *J Neurosci* 18:9620–9628.
5. Kanner BI, Bendahan A (1982) Binding order of substrates to the sodium and potassium ion coupled L-glutamic acid transporter from rat brain. *Biochemistry* 21:6327–6330.
6. Pines G, Kanner BI (1990) Counterflow of L-glutamate in plasma membrane vesicles and reconstituted preparations from rat brain. *Biochemistry* 29:11209–11214.
7. Kavanaugh MP, Bendahan A, Zerangue N, Zhang Y, Kanner BI (1997) Mutation of an amino acid residue influencing potassium coupling in the glutamate transporter GLT-1 induces obligate exchange. *J Biol Chem* 272:1703–1708.
8. Zhang Y, Bendahan A, Zarbiv R, Kavanaugh MP, Kanner BI (1998) Molecular determinant of ion selectivity of a (Na+ + K+)-coupled rat brain glutamate transporter. *Proc Natl Acad Sci USA* 95:751–755.
9. Wadiche JI, Amara SG, Kavanaugh MP (1995) Ion fluxes associated with excitatory amino acid transport. *Neuron* 15:721–728.
10. Fairman WA, Vandenberg RJ, Arriza JL, Kavanaugh MP, Amara SG (1995) An excitatory amino-acid transporter with properties of a ligand-gated chloride channel. *Nature* 375:599–603.
11. Arriza JL, Eliasof S, Kavanaugh MP, Amara SG (1997) Excitatory amino acid transporter 5, a retinal glutamate transporter coupled to a chloride conductance. *Proc Natl Acad Sci USA* 94:4155–4160.
12. Otis TS, Kavanaugh MP (2000) Isolation of current components and partial reaction cycles in the glial glutamate transporter EAAT2. *J Neurosci* 20:2749–2757.
13. Grewer C, Watzke N, Wiessner M, Rauen T (2000) Glutamate translocation of the neuronal glutamate transporter EAAC1 occurs within milliseconds. *Proc Natl Acad Sci USA* 97:9706–9711.
14. Yernool D, Boudker O, Jin Y, Gouaux E (2004) Structure of a glutamate transporter homologue from *Pyrococcus horikoshii*. *Nature* 431:811–818.
15. Koch HP, Larsson HP (2005) Small-scale molecular motions accomplish glutamate uptake in human glutamate transporters. *J Neurosci* 25:1730–1736.
16. Grewer C, Balani P, Weidenfeller C, Bartusel T, Tao Z, Rauen T (2005) Individual subunits of the glutamate transporter EAAC1 homotrimer function independently of each other. *Biochemistry* 44:11913–11923.
17. Leary GP, Stone EF, Holley DC, Kavanaugh MP (2007) The glutamate and chloride permeation pathways are colocalized in individual neuronal glutamate transporter subunits. *J Neurosci* 27:2938–2942.
18. Koch HP, Brown RL, Larsson HP (2007) The glutamate-activated anion conductance in excitatory amino acid transporters is gated independently by the individual subunits. *J Neurosci* 27:2943–2947.
19. Grunewald M, Bendahan A, Kanner BI (1998) Biotinylation of single cysteine mutants of the glutamate transporter GLT-1 from rat brain reveals its unusual topology. *Neuron* 21:623–632.
20. Grunewald M, Kanner BI (2000) The accessibility of a novel reentrant loop of the glutamate transporter GLT-1 is restricted by its substrate. *J Biol Chem* 275:9684–9689.
21. Slotboom DJ, Sobczak I, Konings WN, Lolkema JS (1999) A conserved serine-rich stretch in the glutamate transporter family forms a substrate-sensitive reentrant loop. *Proc Natl Acad Sci USA* 96:14282–14287.
22. Boudker O, Ryan RM, Yernool D, Shimamoto K, Gouaux E (2007) Coupling substrate and ion binding to extracellular gate of a sodium-dependent aspartate transporter. *Nature* 445:387–393.
23. Zhang Y, Kanner BI (1999) Two serine residues of the glutamate transporter GLT-1 are crucial for coupling the fluxes of sodium and the neurotransmitter. *Proc Natl Acad Sci USA* 96:1710–1715.
24. Borre L, Kanner BI (2001) Coupled, but not uncoupled, fluxes in a neuronal glutamate transporter can be activated by lithium ions. *J Biol Chem* 276:40396–40401.
25. Bendahan A, Armon A, Madani N, Kavanaugh MP, Kanner BI (2000) Arginine 447 plays a pivotal role in substrate interactions in a neuronal glutamate transporter. *J Biol Chem* 275:37436–37442.
26. Teichman S, Kanner BI (2007) Aspartate-444 is essential for productive substrate interactions in a neuronal glutamate transporter. *J Gen Physiol* 129:527–539.
27. Pines G, et al. (1992) Cloning and expression of a rat brain L-glutamate transporter. *Nature* 360:464–467.
28. Kanai Y, Hediger MA (1992) Primary structure and functional characterization of a high-affinity glutamate transporter. *Nature* 360:467–471.
29. Arriza JL, Fairman WA, Wadiche JI, Murdoch GH, Kavanaugh MP, Amara SG (1994) Functional comparisons of three glutamate transporter subtypes cloned from human motor cortex. *J Neurosci* 14:5559–5569.
30. Rosental N, Bendahan A, Kanner BI (2006) Multiple consequences of mutating two conserved beta-bridge forming residues in the translocation cycle of a neuronal glutamate transporter. *J Biol Chem* 281:27905–27915.
31. Wadiche JI, Kavanaugh MP (1998) Macroscopic and microscopic properties of a cloned glutamate transporter/chloride channel. *J Neurosci* 18:7650–7661.

32. Grunewald M, Kanner B (1995) Conformational changes monitored on the glutamate transporter GLT-1 indicate the existence of two neurotransmitter-bound states. *J Biol Chem* 270:17017–17024.
33. Otis TS, Jahr CE (1998) Anion currents and predicted glutamate flux through a neuronal glutamate transporter. *J Neurosci* 18:7099–7110.
34. Watzke N, Bamberg E, Grewer C (2001) Early intermediates in the transport cycle of the neuronal excitatory amino acid carrier EAAC1. *J Gen Physiol* 117:547–562.
35. Zhang Z, et al. (2007) Transport direction determines the kinetics of substrate transport by the glutamate transporter EAAC1. *Proc Natl Acad Sci USA* 104:18025–18030.
36. Shrivastava IH, Jiang J, Amara SG, Bahar I (2008) Time-resolved mechanism of extracellular gate opening and substrate binding in a glutamate transporter. *J Biol Chem* 283:28680–28690.
37. Tao Z, Gameiro A, Grewer C (2008) Thallium ions can replace both sodium and potassium ions in the glutamate transporter excitatory amino acid carrier 1. *Biochemistry* 47:12923–12930.
38. Tao Z, Zhang Z, Grewer C (2006) Neutralization of the aspartic acid residue Asp-367, but not Asp-454, inhibits binding of Na+ to the glutamate-free form and cycling of the glutamate transporter EAAC1. *J Biol Chem* 281:10263–10272.
39. Tao Z, Grewer C (2007) Cooperation of the conserved aspartate 439 and bound amino acid substrate is important for high-affinity Na+ binding to the glutamate transporter EAAC1. *J Gen Physiol* 129:331–344.
40. Brocke L, Bendahan A, Grunewald M, Kanner BI (2002) Proximity of two oppositely oriented reentrant loops in the glutamate transporter GLT-1 identified by paired cysteine mutagenesis. *J Biol Chem* 277:3985–3992.
41. Ogawa H, Toyoshima C (2002) Homology modeling of the cation binding sites of Na+K+-ATPase. *Proc Natl Acad Sci USA* 99:15977–15982.
42. Li C, Capendeguy O, Geering K, Horisberger JD (2005) A third Na+-binding site in the sodium pump. *Proc Natl Acad Sci USA* 102:12706–12711.
43. Morth JP, et al. (2007) Crystal structure of the sodium-potassium pump. *Nature* 450:1043–1049.
44. Zarbiv R, Grunewald M, Kavanaugh MP, Kanner BI (1998) Cysteine scanning of the surroundings of an alkali-ion binding site of the glutamate transporter GLT-1 reveals a conformationally sensitive residue. *J Biol Chem* 273:14231–14237.
45. Grewer C, Watzke N, Rauen T, Bicho A (2003) Is the glutamate residue Glu-373 the proton acceptor of the excitatory amino acid carrier 1? *J Biol Chem* 278:2585–2592.
46. Menaker D, Bendahan A, Kanner BI (2006) The substrate specificity of a neuronal glutamate transporter is determined by the nature of the coupling ion. *J Neurochem* 99:20–28.
47. Holley DC, Kavanaugh MP (2009) Interactions of alkali cations with glutamate transporters. *Philos Trans R Soc Lond B Biol Sci* 364:155–161.
48. Borre L, Kanner BI (2004) Arginine 445 controls the coupling between glutamate and cations in the neuronal transporter EAAC-1. *J Biol Chem* 279:2513–2519.
49. Pines G, Zhang Y, Kanner BI (1995) Glutamate 404 is involved in the substrate discrimination of GLT-1, a (Na+ + K+)-coupled glutamate transporter from rat brain. *J Biol Chem* 270:17093–17097.
50. Kunkel TA, Roberts JD, Zakour RA (1987) Rapid and efficient site-specific mutagenesis without phenotypic selection. *Methods Enzymol* 154:367–382.
51. Keynan S, Suh YJ, Kanner BI, Rudnick G (1992) Expression of a cloned gamma-aminobutyric acid transporter in mammalian cells. *Biochemistry* 31:1974–1979.
52. Fuerst TR, Niles EG, Studier FW, Moss B (1986) Eukaryotic transient-expression system based on recombinant vaccinia virus that synthesizes bacteriophage T7 RNA polymerase. *Proc Natl Acad Sci USA* 83:8122–8126.
53. Bennett ER, Su H, Kanner BI (2000) Mutation of arginine 44 of GAT-1, a (Na(+) + Cl(-))-coupled gamma-aminobutyric acid transporter from rat brain, impairs net flux but not exchange. *J Biol Chem* 275:34106–34113.
54. Lowry OH, Rosebrough NJ, Farr AL, Randall RJ (1951) Protein measurement with the Folin phenol reagent. *J Biol Chem* 193:265–275.